Received: 21 March 2018 | Revised: 22 August 2018 | Accepted: 23 August 2018
DOI: 10.1002/mc.22895

RESEARCH ARTICLE

WILEY Molecular Carcinogenesis

Dinitrosopiperazine-decreased PKP3 through upregulating miR-149 participates in nasopharyngeal carcinoma metastasis

Yuejin Li[1,2] | Kunyu Ju[3] | Weiwei Wang[1] | Zheliang Liu[1] | Haitao Xie[4] | Yuan Jiang[1] | Guanmin Jiang[1] | Jinping Lu[2] | Zigang Dong[5] | Faqing Tang[1,2]

[1] Hunan Cancer Hospital and the Affiliated Cancer Hospital of Xiangya School of Medicine, Central South University, Changsha, China

[2] Zhuhai Hospital of Jinan University, Zhuhai, China

[3] Metallurgical Science and Engineering, Central South University, Changsha, China

[4] The First Affiliated Hospital of University of South China, Hengyang, China

[5] Hormel Institute, University of Minnesota, Austin, Minnesota

Correspondence
Faqing Tang, Hunan Cancer Hospital and the Affiliated Cancer Hospital of Xiangya School of Medicine, Central South University, Changsha, China and Zhuhai Hospital of Jinan University, Zhuhai, China.
Email: tangfaqing33@hotmail.com

Funding information
National Natural Science Foundation of China, Grant numbers: 81372282, 81402265, 81402368, 81502346, 81872226

Nasopharyngeal carcinoma (NPC) has a high metastatic clinicopathological feature. As a carcinogen factor, N,N′-dinitrosopiperazine (DNP) is involved in NPC metastasis, but its precise mechanism has not been fully elucidated. Herein, we showed that DNP promotes NPC metastasis through upregulating miR-149. DNP was found to decrease Plakophilin3 (PKP3) expression, further DNP-decreased PKP3 was verified to be through upregulating miR-149. We also found that DNP induced proliferation, adhesion, migration and invasion of NPC cell, which was inhibited by miR-149-inhibitor. DNP may promote NPC metastasis through miR-149-decreased PKP3 expression. Therefore, DNP-increased miR-149 expression may be an important factor of NPC high metastasis, and miR-149 may serve as a molecular target for anti-metastasis therapy of NPC.

KEYWORDS
metastasis, miR-149, nasopharyngeal carcinoma, N,N′-dinitrosopiperazine, Plakophilin3

1 | INTRODUCTION

Nasopharyngeal carcinoma (NPC) is a common malignant cancer in southern China.[1] Epidemiological investigations revealed that incidence of NPC has remained high in endemic regions, particularly in southeast Asia with an incidence of 30-80 per 100 000 people per year.[2,3] In spite of significant advancement in NPC early diagnosis, radiotherapy, surgical intervention and local and systemic adjuvant therapies, the survival rate of five years has not raised significantly. Its main reasons are invasion and distant metastasis which are resistant to available therapies.[4–6]

In endemic NPC, >95% NPC are classified as the undifferentiated World Health Organization (WHO) type III, and are universally associated with Epstein-Barr virus (EBV),[7] genetic factor,[8] and volatile nitrosamine in dietary.[9] Moreover, in studies on Chinese populations in high incidence regions, the relative risk of NPC is also related with their eating habits of the region, especially with dietary intake of salt-preserved fish.[9–16] The

Abbreviations: DNP, N,N′-Dinitrosopiperazine; EBV, Epstein–Barr virus; miRNAs, microRNAs; ncRNA, noncoding RNA; NPC, Nasopharyngeal carcinoma; UTR, untranslated region; PCR, polymerase chain reaction; PKP3, Plakophilin3; TUNEL, TdT-Mediated dUTP Nick End Labeling; VEGF, vascular endothelial growth factor MMP matrix metallo-proteinases.

Yuejin Li, Kunyu Ju, and Weiwei Wang contributed equally to this work.

process of salt preservation is inefficient and becomes partially putrefied, consequently, these foods accumulate significant levels of nitrosamines,[17,18] which are known carcinogens.[17,19,20] N,N′-Dinitrosopiperazine (DNP) is one predominant volatile nitrosamine in salted fish.[14,21] The clinical assay and experiment study have documented that DNP, a specific carcinogen for NPC, is not only involved in NPC carcinogenesis, and but also associate with NPC metastasis.[22–24] Furthermore, DNP has been approved to increase NPC metastasis through inducing Ezrin phosphorylation and HSP70-2, AGR2, Clusterin expression.[25–27]

MicroRNAs (miRNAs) are genome-derived noncoding RNA (ncRNA) molecules that govern target gene expression in a sequence-specific manner.[28,29] They usually bind with partial complementarity to the 3′ untranslated region (3′-UTR) of the corresponding target mRNA. These bindings either cause target mRNA degradation or translational repression, which would lead to activation or inhibition of downstream signaling pathways. miRNAs are revealed to play critical roles in the control of cancer processes including proliferation, cell cycle, apoptosis, invasion, tumorigenesis, and metastasis. This provides a novel clue for miRNA-based therapies. miRNAs are aberrantly expressed in NPC cells and tissues, and involved in the regulation of tumor genes.[30,31] Therefore, investigation of miRNA regulating pathways may offer insights into identification of new NPC oncotargets and development of new therapeutics.[32,33]

miR-149 was reported to be down-regulated in various cancer, negatively correlated with cancer WHO grade.[34–37] Overexpression of miR-149 inhibits glioblastoma cell proliferation and migration.[37] miR-149 has also been proved to inhibit the proliferation and cell cycle progression in human gastric cancer.[38] miR-149 lowly expresses in some tumors, but highly expresses in other tumors. Various tumors have different miR-149 expressions, which may be decided by tumor heterogeneity. The upregulated miR-149 was reported in NPC tissue[39] and cell lines.[40] miR-149 had been confirmed to promote the proliferation, invasion and migration of NPC cell,[41] but its regulating mechanism is not clear. Moreover, a target scan analysis revealed that 3′-UTRs of Plakophilin3 (*Pkp3*) gene retains binding sites for miR-149, this implies that *Pkp3* is a target gene of miR-149. PKP3 is a desmosomal plaque protein that belongs to p120 catenin subfamily of the armadillo family, and is found in desmosomes of most epithelial tissues with the exception of hepatocytes.[42] PKP3 loss was associated with tumor progression and metastasis in oral cavity and colon tumors.[43,44] Our previous works showed that PKP3 expression is decreased in DNP-induced NPC metastasis.[45] In this article, we found that DNP induced NPC metastasis, conjugating the increased expression of miR-149 and the decreased PKP3, while miR-149-inhibitor decreased DNP-induced NPC metastasis through upregulating PKP3 expression. We think that DNP induces NPC metastasis through miR-149 downregulating PKP3 expression. These provide novel clues for NPC metastasis research.

2 | MATERIALS AND METHODS

2.1 | Cell cultures and treatment

Human NPC cell lines, 6-10B and 5-8F are sublines derived from cell line SUNE-1, were obtained from Sun Yat-sen University Cancer Center (Guangzhou, China). 6-10B has a low metastatic ability, while the 5-8F has a high metastatic ability[25] (cell line authentication is showed in Supplemental Material). These cells were incubated in Dulbecco's Modified Eagle Medium (DMEM) containing 10% fetal bovine serum (FBS), L-glutamine, 100 IU/mL penicillin, 100 mg/mL streptomycin, and 0.25 mg/mL amphotericin (Life Technologies, Bethesda, MD) at 37°C in a humidified atmosphere of 5% CO_2.[46] The cells in logarithmic growth were inoculated in a 12-well culture plate (3×10^5 cells/well). The cell wells were divided into four groups: i) Sham group without any treatment (BC); ii) Treatment with DNP plus mock microRNA (DNP+NC); iii) Treatment with DNP plus miR-149 (DNP+miR-149); iv) Treatment with miR-149 (miR-149). DNP crystals were dissolved in DMSO as DNP stock solution, and appropriate amounts of DNP stock solution were added to the culture cells to achieve the indicated concentrations. Opti-MEM culture medium containing miR-149 and mock microRNA was respectively used to transfect cells. Subsequently, interferon was added to improve transfection efficiency. Final concentrations of miR-149 and mock miRNA in each well were 20 nmol/L with at 4 μL, and transfected for 72 h. The experiments were repeated three times.

2.2 | Antibodies and Western-blotting analysis

Antibody against PKP3 was purchased from Abcam (Cambridge, UK). Antibody against GAPDH was purchased from kangchen Inc. (Shanghai, china). The secondary antibodies were purchased from Santa Southern Biotech, Inc. (Birmingham, USA). Western-blotting analysis was performed as previously described.[45] Briefly, after DNP treatment and gene transfection, the treated cells were disrupted with lysis buffer (1 × PBS, 1% Nonidet P-40, 0.5% sodium deoxycholate, 0.1% SDS, and freshly added 100 μg/mL PMSF, 10 μg/mL aprotinin, and 1 mM sodium orthovanadate). The cell lysates were subjected to centrifugation to obtain the supernatant. The protein concentration of supernatant sample was determined using the Bio-Rad Protein Assay (Bio-Rad Laboratories, Inc., Hercules, CA). Protein from supernatant sample was separated by electrophoresis, and transferred onto a nitrocellulose membrane. The protein membrane was incubated with specific antibody against PKP3, and then incubated with the peroxidase-conjugated secondary antibody. The signal was developed using 4-chloro-1napthol/3,3-o-diaminobenzidine. The relative photographic density was quantified by scanning the photographic negative using a gel documentation and analysis system. GAPDH was used as an internal control to verify basal level expression and equal protein loading. The abundance ratio to GAPDH was counted.

2.3 | NPC biopsy samples

A total of 175 pathological specimens were collected from January 2011 to June 2015 at First and Second Hospital of Nanhua University (Hengyang, Hunan, China) including 144 cases of primary NPC tissues and 31 cases of normal nasopharyngeal (NNP). All specimens were confirmed by histopathological examination. None of the patients underwent chemotherapy or other adjuvant therapy. A total of 144 patients with NPC were comprised of 108 men and 36 women with age from 20 to 71 years

(median, 43.6 years). A total of 31 cases of NNP included 17 men and 14 women with age range between 17 and 65 years (mean age 43.3 years).

2.4 | Immunohistochemistry

Immunohistochemistry was performed on tissue sections of NPC specimens and metastatic tumors according to the methods described previously with minor modifications.[46] Briefly, tissue sections were stained with hematoxylin and eosin for microscopic examination. The unstained sections were used for staining with antibody against PKP3 by immunohistochemistry. Immunohistochemistry was performed following standard procedures with overnight exposure at room temperature at 1:500 PKP3 antibody diluted in 0.5% nonfat milk. After being washed with phosphate-buffered saline (PBS), the sections were incubated sequentially with the secondary antibody against mouse at 1:1000, peroxidase enzyme label and diaminobenzidine (Sigma), stained with hematoxylin (Polysciences, Inc., Warrington, PA), dehydrated, and mounted under a glass cover slip. Sections stained with normal mouse IgG served as a negative control.

The sections were evaluated by two investigators without prior knowledge of the clinical data, independently graded the staining intensity in all cases. PKP3 staining was assessed according to the methods described by Li[26] with minor modifications. Each case was scored based on the intensity and percentage of cells. At least 10 high-power fields were chosen randomly, and >1000 cells were counted for each section. The intensity of PKP3 staining was scored as 0 (no signal), 1+ (weak), 2 (moderate), and 3 (marked). Percentage scores were assigned as 0, 0-25%; 1, 26-50%; 2, 51-75%; and 3, 76-100%. The summed (extension + intensity) was used as the total score. We grouped all samples into the high expression group (total score ≥2) and the low one (total score <2) according to the protein expression.

2.5 | miRNA sequencing analysis

After being treated with DNP at 80.0 μmol/L for 24 h,[26] 6-10B cells were harvested, total RNA was extracted using TRIzol reagent (Invitrogen). Thirty to fifty milligrams total RNA was determined with an ND-1000 spectrophotometer (NanoDrop Technologies Inc., Wilmington, DE, USA). Small RNA library construction was performed as described.[47] Briefly, 15-30 nt small RNAs were isolated on 15% PAGE (7 M urea), and ligated to the 5′ and 3′ RNA adaptors. RT-PCR using primers with partial complementarity to the adaptors were performed. Four DNA pools from different samples were amplified from the first-strand cDNA and then sequenced using Hiseq2000 (Illumina, USA) at Beijing Genomics Institute at Shenzhen according to the manufacturer's protocol, and novel miRNAs were predicted as described.[47] The experiments were performed in triplicate.

2.6 | RT-PCR

RT-qPCR with gene-specific primers for SYBR® Green reporter was conducted as previously described.[26] Briefly, total RNA was isolated using Trizol (Invitrogen Co., Shanghai, China) reagent following the manufacturer's instructions. The resultant RNA was reverse-transcribed to cDNA using a PrimeScript® RT Master Mix kit (Takara Co., Dalian, China). Gene-specific primers were combined with SYBR® Premix Ex Taq™ (Takara) and amplified using an ABI 7500 Real-Time PCR System (Applied Biosystems, Foster City, CA). All qPCR reactions were independently conducted on five samples with prime sequence shown in Table 1. The relative mRNA expression levels were calculated using the $2^{-\triangle\triangle Ct}$ method.

2.7 | Luciferase activity assay

3′ untranslated region (UTR) of *Pkp3* gene, which contains miR-149 binding sites, was amplified using PCR with prime sequence shown in Table 2 and was cloned into the downstream of psiCHECK-2 luciferase vector (Promega, Madison, WI), named as wt 3′UTR. The binding site was intentionally mutated using the GeneTailor Site-Directed Mutagenesis System (Invitrogen), and the resultant mutant 3′UTR was cloned into the same vector, named as Mut 3′ UTR. 6-10B cells maintained in 48-well plates were co-transfected with wt 3′UTR or Mut 3′ UTR plasmid construct and miR-149 mimics or control miRNA using Lipofectamine 2000 (Invitrogen). The transfected cells were analyzed by the Dual-Luciferase Reporter Assay System (Promega) 48 h after their transfection following the manufacturer's instructions.

2.8 | Cell growth curve analysis and colony forming assay

According to the previous works, cell growth curve and colony of the treated cells were detected.[48] Briefly, the treated cells were

TABLE 1 Primer sequences for RT-qPCR

Gene	Sequence (5′-3′)
PKP3	Forward:TGAGCCACCTGATCGAGAA
	Reverse:GGTTGTTGAGCACAGCTATGA
18srRNA	Forward:CCTGGATACCGCAGCTAGGA
	Reverse:GCGGCGCAATACGAATGCCCC
U6	Forward:CTCGCTTCGGCAGCACA
	the stem-loop RT:AACGCTTCACGAATTTGCGT
miR-149	Forward:ATGGTTCGTGGGTCTGGCTCCGTGTCTTCA the stem-loop RT:GTCGTATCCAGTGCAGGGTCCGAGGTATTCGCACTGGATACGACCGGGAGTGA

TABLE 2 Primer sequences for luciferase reporter

Gene	Sequence (5′-3′)	
Pkp3 wt 3′ UTR	Sence	CCGCTCGAGCACCTTCTCCTCCAGAAGGCTTCAC
	Antisence	ATAAGAATGCGGCCGCTGGGAATAAAGATGGCCATGAACAGTCA
Pkp3 mut 3′ UTR	Sence	GCCTGGCAGTATCTTGGGATCTGGCTCACTGGGAATAAAGATGGCCAT
	Antisence	ATGGCCATCTTTATTCCCAGTGAGCCAGATCCCAAGATACTGCCAGGC

trypsinized and counted. For growth curve analysis, the cells were incubated in the well of 12-well plates in triplicate, were cultured in growth media, and were counted with Coulter counter (Beckman Coulter, Inc.). Proliferation efficiency (%) = (OD value in experimental well − OD value of control well)/OD value of control well × 100%. For colony forming assay, the cells were cultured in a 96-well culture plate at 1×10^3 cells/well. After being cultured for 7 days, the cell wells were stained with crystal violet, the number of cell colonies was calculated for three times. The colony formation efficiency (%) was calculated as the ratio of the number of colonies to the number of inoculated cells.

2.9 | Cell adhesion assay

Cell adhesion ability of the treated cells were detected using Cell adhesion assay according to the methods described previously with minor modifications.[49] Briefly, ninety-six-well dishes were pre-coated with 30 mg/L fibronectin solution (50 μL/well), then air-dried at room temperature overnight. The cell wells were rinsed with PBS, and incubated with 3% heat-denatured bovine serum albumin (BSA) to block any uncoated areas. Two hundred microliters of cell suspension (0.5×10^6 cells) were seeded in the coated wells, and incubated for 60 or 90 min at 37°C. The non-adherent cells were removed by washing with PBS. DMEM containing 10% FBS was added to each well, and cells were then incubated at 37°C for 4 h. Next, 10 μL of CellTiter 96 AQueous One Solution (Promega) was added to each well, and cells were incubated for an additional 4 h at 37°C. Absorbance was measured at 490 nm using a microplate reader (Multiskan MK3, Thermo Scientific, Vantaa, Finland).

2.10 | Cell invasion and migration assay

Boden chamber invasion assay was performed with minor modifications as described previously by Tang et al.[25] Briefly, the transfected cells were treated with 0.2% trypsin, the treated cells were suspended. The migration of the treated cells was directly tested using Boyden chamber. For invasion assay, Boyden chambers were coated with Matrigel (BD, Bedford, MA) at 25 mg/50 mL, the suspended cells were seeded into the coated Boyden chamber and the uncoated Boyden chamber in the upper part at a density of 1.5×10^4 cells/well in 50 μL of serum-free medium, and then incubated for 12 h at 37°C. The bottom chamber was added standard medium containing 20% FBS. The cells invaded to the down surface of membrane were fixed with methanol, and stained with crystal violet. The invaded cells were counted under microscope at 200 × magnification. The numbers of cell migration and invasion were calculated.

2.11 | Flow cytometric analysis

Cell apoptosis was detected by flow cytometry according to the previous describing.[50] Briefly, the treated cells were analyzed by flow cytometry using an Annexin V-FITC Apoptosis Detection Kit (KeyGEN Biotech, Nanjing, China). According to the manufacturer's protocol, Annexin V-FITC (1.25 μL) and propidium iodide (PI) (10 μL) were added to 500 μL of the cell suspension (5×10^5 cells/mL) in binding buffer. The flow cytometry data were analyzed using an LSRII flow cytometer (BD calibur, San Jose, CA) according to the manufacturer's instructions. All experiments were performed in triplicate.

2.12 | Mitochondrial membrane potential assay

ΔΨm (mitochondrial membrane potential) was assessed using a flow cytometer (BD calibur). Briefly, the treated cells were stained with 5,5′,6,6′-tetraethyl-benzimidazolylcarbocyanine iodide (JC-1) dye (Life Technologies Corporation) according to the manufacturer's instructions. The cells were cultured according to the corresponding groups and were stained with JC-1 for 20 min at 37°C in a CO_2 incubator. Green fluorescence was analyzed in the FL-1 (FITC) channel and red fluorescence was analyzed in the FL-2 (PE-A) channel. The fluorescence intensity was acquired for 10 000 events. The ratio of red (JC-1 polymer) to green fluorescence (JC-1 monomer) intensity was determined for each sample as a measure of ΔΨm.

2.13 | TdT-mediated dUTP nick end labeling (TUNEL) assay

To determine the percentage of apoptotic cells in the treated cells, we performed terminal deoxynucleotidyl transferase-mediated dUTP nick-end labeling assay (TUNEL) staining using the DeadEnd™ Fluorometric TUNEL System (Promega). First, the treated cells were cultured according to the corresponding groups, and then fixed with 4% paraformaldehyde in PBS for 10 min at room temperature. After being washed with PBS, the cell slides were permeabilized with 0.5% Triton X-100 in 0.1% sodium citrate for 20 min. The slides were pre-balanced by buffer for 10 min, and covered with TUNEL reaction mixture in a dark room at 37°C for 1 h, and then treated with termination by 2 × SCC converter at room temperature for 15 min. After being washed, the slides were incubated with 4′,6-diamidino-2-phenylindole (DAPI) for 10 min at room temperature, and then washed and mounted in a fluorescence protector medium. The slides were

evaluated using fluorescence microscopy. The number of green cells among 500 cells was counted. Three samples from each group were analyzed.

2.14 | Tube formation assay

The tube formation assay was conducted as the described methods with minor modifications.[51] Briefly, 6-10B cells were transfected with miR-149, and incubated in medium with or without DNP for 24 h, and then 2 mL of the conditioned medium was collected. For tube formation assay, 96-well plate was coated with Matrigel (BD Biosciences, USA) and kept in 37°C for 2 h. Then, 2×10^4 HUVECs (Human Umbilical Vein Endothelial Cells) were suspended in 100 mL of the conditioned medium, and added to the precoated 96-well plate. After incubation at 37°C for 24 h, the cell growth was taken photographs under microscope, and the tubular structures formed were counted. The experiments were performed in triplicate, and five fields from each chamber were counted and averaged.

2.15 | F-actin staining

The treated cells were fixed with 4% paraformaldehyde for 15 min at room temperature, and incubated with phalloidin (5 μg/mL) at room temperature for 1 h, and then stained with DAPI for 10 min. The coverslips were mounted in Mowiol mountant (Calbiochem, Merck, Germany), and images were captured using TCS SP2 AOBS confocal microscope (Leica Microsystems Inc., Buffalo Grove, IL). The fluorescence intensity was measured in 10 fields/well using ImageJ software and divided by the DAPI counts. The transfections or treatments were performed in duplicate, and experiments were repeated ≥3 times.

2.16 | Animals

Twenty female nude BABL/c mice (approximately 5-6 weeks old) were purchased from the Animal Center of Central South University. They were maintained under laminar airflow conditions in the Laboratory for Experiments, Central South University. The studies were conducted according to the standards established by the Guidelines for Care and Use of Laboratory Animals of Central South University.

2.17 | Evaluation of the effect of DNP and miR-149 on NPC metastasis in nude mice

The effects of miR-149 on 5-8F and DNP-induced 6-10B cell metastasis were determined in vivo as described previously with some modifications.[25] Briefly, 100 μL (10×10^4) of 5-8F cells transfected with miR-149-inhibitor were mixed with 100 μL (5 mg/mL) Matrigel, and respectively injected into the tail veins of nude mice (10 mice/group). After 30 days, metastasis was evaluated by measuring the metastatic node numbers and the weight of metastasized tumors. 6-10B cells were treated with miR-149-inhibitor, and then injected into 20 nude mice. The injected mice were randomly divided into two groups with 10 mice per group. One group was abdominally injected with DNP at a dosage of 40 mg/kg (body weight) twice a week for 30 days. The other group was injected with saline. After 30 days, the mice were sacrificed and dissected, metastatic tumors were observed under anatomical microscope. The present study protocols were approved by the ethical committees at Zhuhai Hospital of Jinan University and Xiangya Hospital of Central South University.

2.18 | Statistical analysis

Data analysis was performed using SPSS version 18.0 software (SPSS, Inc., Chicago, IL). The results are expressed as the mean ± standard error of the mean from a minimum of three independent experiments. The statistical significance between groups was determined by one way analysis of variance. $P < 0.05$ was considered to indicate a statistically significant difference.

3 | RESULTS

3.1 | Differentially expressed miRNAs in DNP-treated 6-10B cells

DNP is a specific pathogenic factor for NPC, its structure is showed Figure 1A. Our previous works showed that DNP induced NPC metastasis.[25,26] In this experiment, we want to screen microRNAs in DNP-induced NPC metastasis. miRNA sequencing was used to screen different expression miRNAs. The results showed that the differential miRNAs in DNP treatment and untreatment chips did not overlap. After multiple rescreening processes, the miRNAs modulated by DNP were identified using a miRNA microarray (Table 3, Figure 1B). miR-3687, miR-1291, miR-338-3p, miR-486-3p, hsa-miR-149, hsa-miR-5088-5p, hsa-miR-1276, and hsa-miR-642a-3p highly expressed in DNP-treated cells, and miR-1307-3p, miR-29b-1-5p, miR-1273d, miR-4741, miR-6889-5p, miR-660-3p, miR-1246, miR-500a-5p, hsa-miR-500b-5p were low expression. Based on miR-149's role in tumor cell proliferation and migration,[52,53] we focused on that miR-149 involves in NPC metastasis. miR-149 expression level was confirmed using qRT-PCR. The data showed that miR-149 expression was significantly higher in DNP-treated cells than that in the control (Figure 1C, $P < 0.05$), it is consistent with sequencing data. These indicated that DNP induces miR-149 expression. We also found that miR-149 was significantly increased in NPC tissues compared to the adjacent normal NP tissues (Figure 1D, $P < 0.05$). This data showed that miR-149 is associated with NPC progress.

3.2 | MiR-149's effect on *PKP3* transcription and PKP3 expression in NPC tissues

A target scan analysis revealed that 3′-UTRs of *Pkp3* exists binding sites for miR-149 (Figure 2A). Vectors containing the potential binding sites or its mutation were constructed (Figure 2A). Luciferase activity assay was used to confirm the regulation of miR-149 to *Pkp3 gene*.

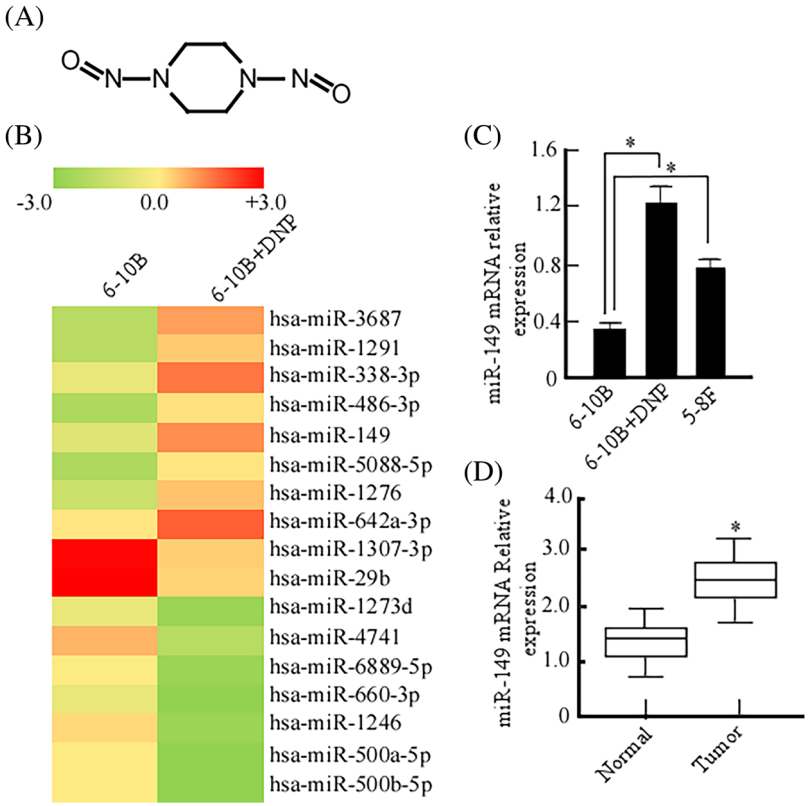

FIGURE 1 DNP upregulates miR-149 expression. A, Structure of DNP, a N-nitroso compound. B, miRNA sequencing was used to construct miRNAs expression profiles of DNP-treated 6-10B cells and the untreated. Red represents high expression, and green is low expression. C, miR-149 was detected using qRT-PCR in 6-10B cells treated with DNP and the untreated cells, and 5-8F cells served as a positive control. D, The expression of miR-149 was detected in the tumors and paired adjacent tissues from NPC patients. DNP, Dinitrosopiperazine. *$P < 0.05$

TABLE 3 Different miRNAs selected by miRNA sequencing analysis

miRNA name	Fold-change(log_2 DNP-treated 6-10B /6-10B)	Direction
hsa-miR-3687	1.99054941	Upregulated
hsa-miR-1291	1.57553179	Upregulated
hsa-miR-338-3p	1.53493711	Upregulated
hsa-miR-486-3p	1.49316733	Upregulated
hsa-miR-149	1.48543761	Upregulated
hsa-miR-5088-5p	1.40571063	Upregulated
hsa-miR-1276	1.28015129	Upregulated
hsa-miR-642a-3p	1.27602206	Upregulated
hsa-miR-1307-3p	−1.54133701	Downregulated
hsa-miR-29b-1-5p	−1.54278560	Downregulated
hsa-miR-1273d	−1.59439373	Downregulated
hsa-miR-4741	−1.78703880	Downregulated
hsa-miR-6889-5p	−1.81674665	Downregulated
hsa-miR-660-3p	−2.00943123	Downregulated
hsa-miR-1246	−2.17935623	Downregulated
hsa-miR-500a-5p	−2.33135932	Downregulated
hsa-miR-500b-5p	−2.33135932	Downregulated

The results showed that the transcript activity of *Pkp3* gene was significantly decreased when being transfected with miR-149 (Figure 2B, $P < 0.05$). Nonetheless, in mutation of 3′ UTR, there was no significant difference between the transfected with miR-149 and the vector control (Figure 2B). Next, we further detected PKP3 expression in NPC biopsy tissues using immunohistochemistry. As shown in Figure 2C, PKP3 was localized in nucleus, cytoplasm and intercellular, and positive signals showed brown-yellow granules (Figure 2C-a). Furthermore, PKP3 was significantly decreased in NPC tissues compared to the adjacent tissues (Figure 2C-b, $P < 0.05$). And the relationship of PKP3 expression with clinicopathological features was shown in Table 4. PKP3 expression was negatively correlated with T stage (original tumor size and nearby tissue invasion) (Figure 2C-c; $P < 0.05$), N stage (lymph node metastasis) (Figure 2C-d; $P < 0.01$), and M stage (distant metastasis), respectively (Figure 2C-e; $P < 0.01$). Low expression of PKP3 is associated with NPC progress.

3.3 | DNP decreases PKP3 and increases miR-149 expression

To investigate whether DNP affects PKP3 and miR-149 expression, 6-10B cells were treated with 0-80.0 μmol/L DNP for 24 h for dose-course assays or with 80.0 μmol/L DNP for 0-24 h for time-course assay, and then PKP3 expression were detected using

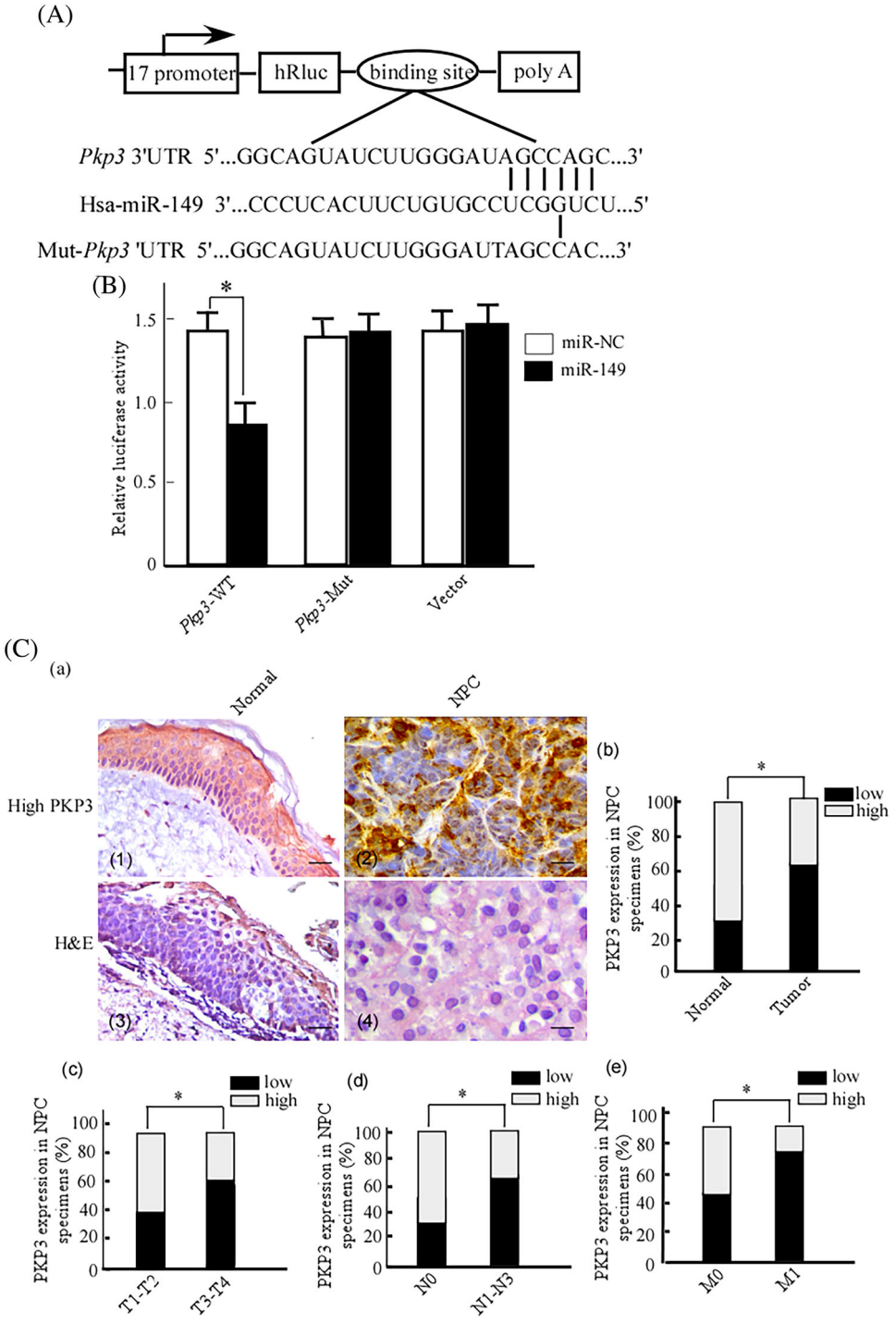

FIGURE 2 Analysis of miR-149 binding to PKP3 and PKP3 expression in NPC specimens. A, Putative targets predicted by TargetScan. B, Transcript activity of *Pkp3* gene in the cells transfected with miR-149 was detected using luciferase activity assay. 3′untranslated region (UTR) of *Pkp3* gene and Mut-UTR were amplified using PCR, and respectively cloned into the downstream of psiCHECK-2 luciferase vectors. These vectors were cotransfected into 6-10B cells with miR-149 or miR-NC. The transfected cells were analyzed by the Dual-Luciferase Reporter Assay System. NC, non-targeting control; WT, wild-type; Mut, mutation. C, PKP3 expression was detected in NPC specimens and the paired adjacent tissues using immunohistochemistry (a). b, c, d, and e, graphical illustration of PKP3 expression in NPC specimens. T, original tumor and nearby invasion; N, lymph node metastasis; M, distant metastasis. scale bar, 100 μm; PKP3, Plakophilin3. Original magnification, ×400. *$P < 0.05$

TABLE 4 The relationship of PKP3 expression with clinicopathological features

Characteristic	Cases	PKP3 expression		P
		Low	High	
All patients				
Gender				
Male	108	54 (50.0%)	54 (50.0%)	1.000
Female	36	17 (47.2%)	19 (52.8%)	
Age (yrs)				
<50	80	40 (50.0%)	40 (50.0%)	1.000
≥50	64	31 (48.4%)	33 (51.6%)	
T stage				
T1-T2	60	24 (40.0%)	38 (60.0%)	0.011
T3-T4	84	50 (59.5%)	34 (40.5%)	
N stage				
N0	60	21 (35.0%)	39 (65.0%)	0.000
N1-N3	84	56 (66.7%)	28 (33.3%)	
M stage				
M0	126	62 (49.2%)	64 (50.8%)	0.006
M1	18	15 (83.3%)	3 (16.7%)	

Western-blotting, miR-149 expression was detected using qRT-PCR. After 6-10B cells being treated with DNP, PKP3 expression dramatically decreased (Figure 3A-a, b; 3B-a, b; $P < 0.05$) and miR-149 expression drastically increased, and displayed a dose- and time-dependently manner (Figure 3A-c, B-c; $P < 0.05$). These findings indicated that DNP decreases PKP3 expression and increases miR-149 expression. Compared with 6-10B with low metastatic ability, 5-8F cells with high metastatic ability had a relative low expression of PKP3 (Figure 3A-a, b, lane 4 vs 1 in upper panel; $P < 0.05$) and a relative high expression of miR-149 (Figure 3A-c, lane 4 vs 1; $P < 0.05$).These results imply that the decreased PKP3 and increased miR-149 mediated by DNP may be involved in NPC metastasis.

3.4 | DNP increases 6-10B cells proliferation through miR-149

6-10B cell has a low malignant phenotype[25,26] and low miR-149, it was used to investigate whether miR-149 is involved in DNP-induced malignant phenotype. To observe the role of miR-149 in DNP-mediated 6-10B malignant phenotype, we used miR-149-inhibitor to decrease miR-149 expression, and detected cell proliferation and colony growth. The results showed that the cell proliferation of DNP-treated group significantly increased (Figure 4A). Compared to NC (non-targeting control, NC) group, miR-149-inhibitor dramatically decreased DNP-increased 6-10B cell proliferation (Figure 4A). We further evaluated the effect of DNP on 6-10B cells colony formation. The colony-forming efficiency (CFE) values of NC, 6-10-miR-149, 6-10B-DNP, and 6-10B-DNP-miR-149-inhibitor were 12 ± 2.1%, 5% ± 1.8%, 29 ± 2.1%, 13 ± 2.3%, respectively. DNP-treated 6-10B cells statistically exhibited high CFE (Figure 4B, $P < 0.01$), and 6-10B-miR-149-inhibitor exhibited low CFE when compared with NC cells (Figure 4B, $P < 0.05$). These data show that DNP induces cell growth and colony-forming through miR-149 high expression.

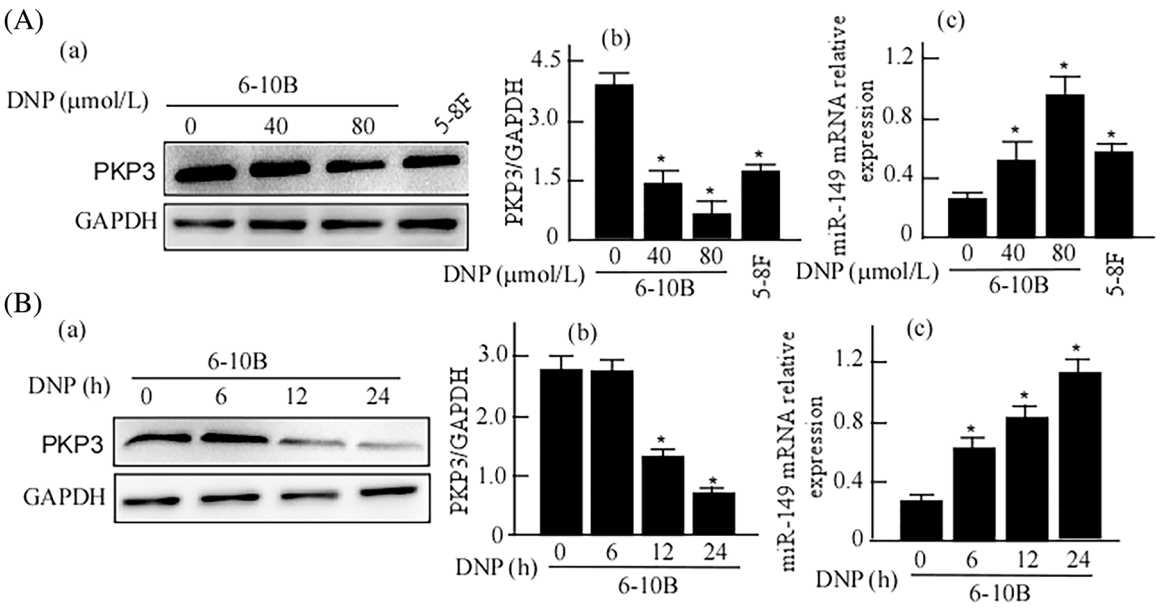

FIGURE 3 Expressions of PKP3 and miR-149 in 6-10B cells with DNP treatment. A, 6-10B cells were treated with the indicated concentration of DNP for dose-course. B, 6-10B cells were treated with DNP for the indicated time for time-course. PKP3 in the treated cells was detected using Western-blotting (a). GAPDH was used as an internal control. The abundance ratio of PKP3 to GAPDH was counted for PKP3 quantitative analysis (b), and miR-149 expression was detected using qRT-PCR (c). DNP, Dinitrosopiperazine; PKP3, Plakophilin3. *$P < 0.05$

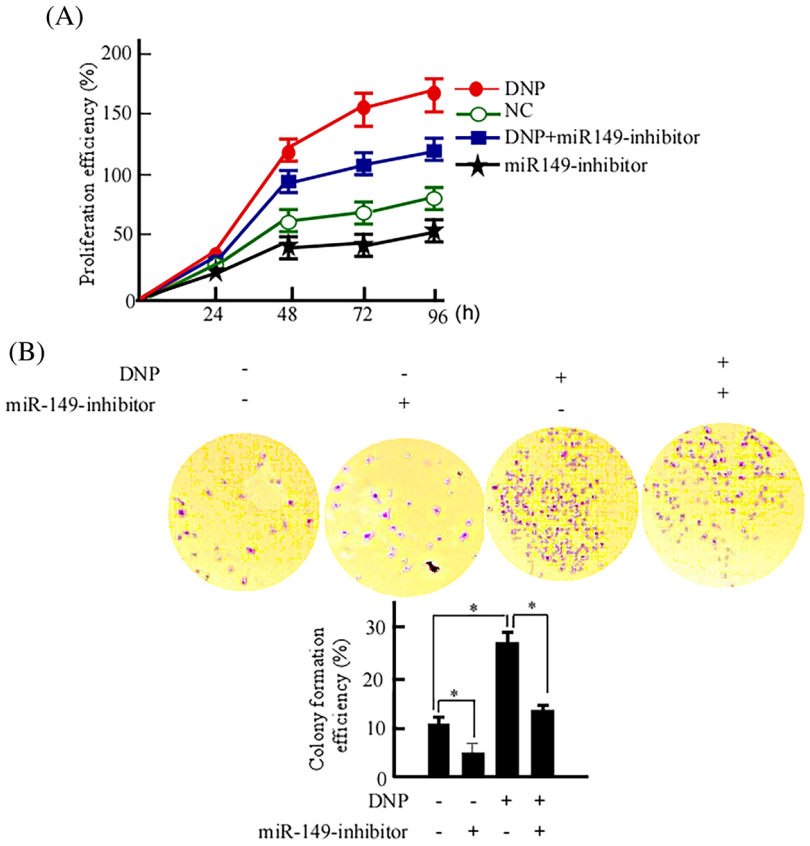

FIGURE 4 miR-149 inhibits DNP-induced proliferation and colony growt. A, 6-10B cells were treated with DNP, DNP plus miR-149-inhibitor or miR-149-inhibitor, respectively. Viability of the treated cells was measured using MTT. The growth curves of the treated cells were calculated. NC, non-targeting control. B, colony-forming of 6-10B cells treated with DNP, DNP plus miR-149-inhibitor, or miR-149-inhibitor using colony formation assay. DNP, Dinitrosopiperazine. *$P < 0.05$

3.5 | DNP induces NPC cell migration, invasion, and adhesion through miR-149

Our previous works have shown that DNP can induce NPC cell migration and invasion.[45] To determine the role of miR-149 in DNP-induced cell migration and invasion, transwell cell assays were used to detect the migration and invasion of 6-10B cells with DNP treatment and miR-149 transfection. Adhesion assays were performed to determine the role of miR-149 on DNP-induced cell adhesion. Compared with the blank control, migration and invasion of 6-10B cells were dramatically decreased when treated with miR-149-inhibitor (Figure 5B-b, f, m, n; $P < 0.05$). DNP treatment significantly increased 6-10 cell invasion and migration (Figure 5B-c, g, m, n; $P < 0.05$), and this increase was partly inhibited by miR-149-inhibitor (Figure 5B-d, h, m, n; $P < 0.05$). Adhesion assays result was consistent with the transwell, the adhesion ability of 6-10B cells with miR-149-inhibitor was significantly weaker than that of the blank control (Figure 5B-j, o; $P < 0.05$), and DNP-induced adhesion ability was dramatically decreased when being treated with miR-149-inhibitor (Figure 5B-l, o; $P < 0.05$). Simultaneously, DNP-mediated PKP3 expression was also significantly decreased in 6-10B cells (Figure 5A-a, b; $P < 0.05$), and the effect was dramatically attenuated when miR-149 expression was inhibited (Figure 5A-a, b; $P < 0.05$). Moreover, the cell invasion and migration of 5-8F cells were decreased when being transfected with miR-149-inhibitor (Figure 5D-c, f, g, h; $P < 0.05$). Taken together, the data indicate that DNP increases miR-149 and decreases PKP3 expression, and DNP may promote NPC cell invasiveness, migration and adhesion through upregulating miR-149 expression.

3.6 | DNP mediates apoptosis inhibition through regulating miR-149

The above results showed that downregulated-miR-149 inhibits cell growth and colony formation induced by DNP. The next step is to probe whether miR-149 downregulation induces cell apoptosis. The treated cells were stained using Annexin V-FITC/PI, and then were analyzed by flow cytometry. Data showed that the percentage of apoptotic cells significantly increased in 6-10B cells transfected with miR-149-inhibitor (29.2 ± 4.2%) when compared with the blank control (13.8 ± 3.6%) (Figure 6B-b, e; $P < 0.05$). The cells treated with DNP showed a low percentage of apoptosis cells (8.6 ± 1.6%), and this effect was significantly attenuated when miR-149 expression was silenced (14.2 ± 1.8%) (Figure 6B-d, e; $P < 0.05$). To further investigate whether DNP-mediated apoptosis inhibition is associated with mitochondrial, ΔΨm (mitochondrial membrane potential) in the treated

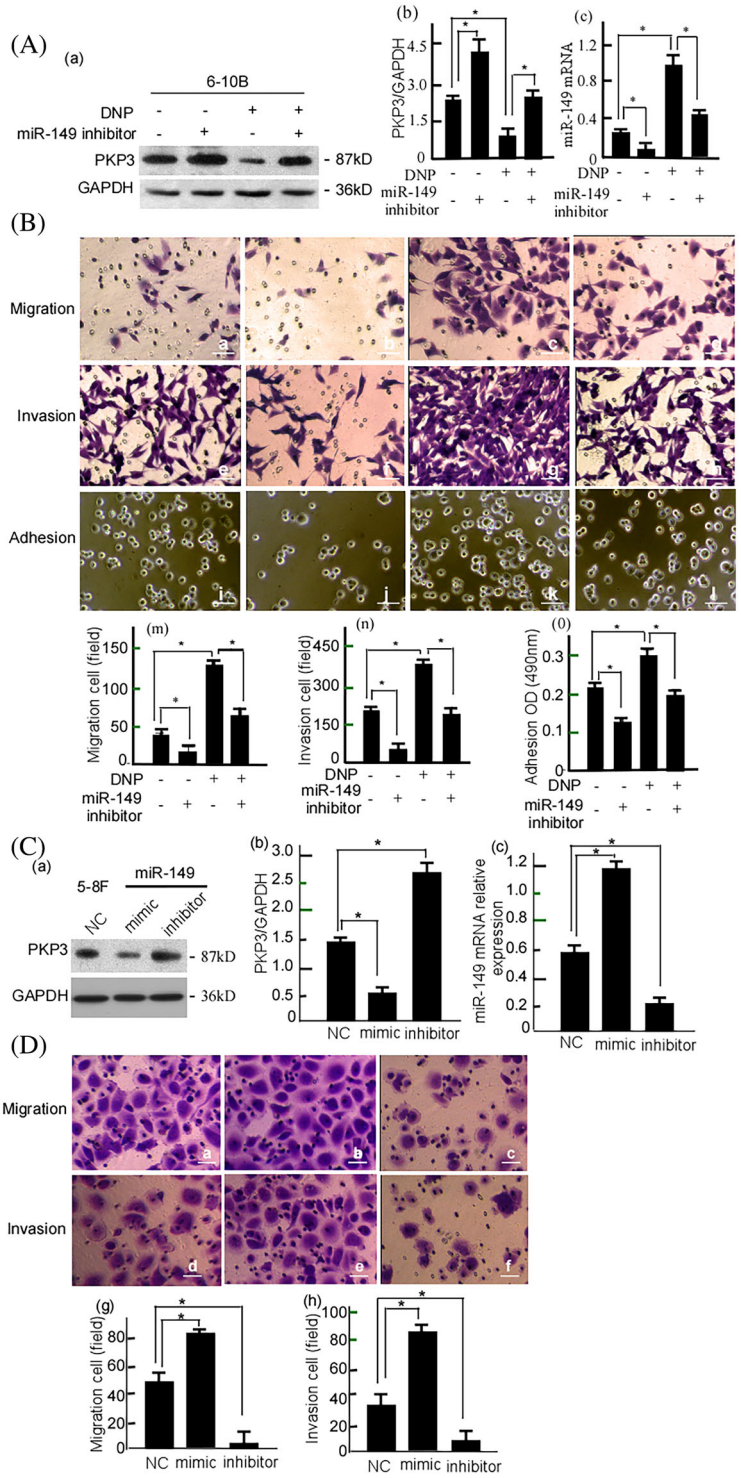

FIGURE 5 DNP-induced NPC cell migration, invasion, and adhesion through miR-149. A, 6-10B cells were treated with miR-149-inhibitor and/or DNP, PKP3 expressions in the treated cells were detected using Western-blotting (a), GAPDH was used as an internal control. The abundance ratio of PKP3 to GAPDH was counted (b), and miR-149 expression was detected using qRT-PCR (c). B, The migration (a-d) and invasion (e-h) of the treated 6-10 cells were detected using Boden chamber assay, and the adhesion (i-k) was detected using Cell adhesion assay. a, e, and i, Blank control; b, f, and j, miR-149-inhibitor treatment; c, g, and k, DNP treatment; d, h, and l, DNP plus miR-149-inhibitor. Cell migration (m), invasion (n), and adhesion (o) was quantitatively analyzed. C, 5-8F cells were treated with mimic or miR-149-inhibitor. PKP3 in the treated cells was detected using Western-blotting (a) and quantitatively analyzed (b), and miR-149 mRNA were detected using qRT-PCR (c). D, Migration (a-c) and invasion (d-f) of the treated 5-8F cells were measured using Boden chamber assay. a and d, Blank control; b and e, Mimic treatment; c and f, miR-149-inhibitor. Data are presented as means ± S.D. from three independent experiments statistically using the Student's *t* test. Scale bar, 5 μm; Original magnification, ×200. NC, Non-targeting control; DNP, Dinitrosopiperazine; PKP3, Plakophilin3. $^{*}P < 0.05$

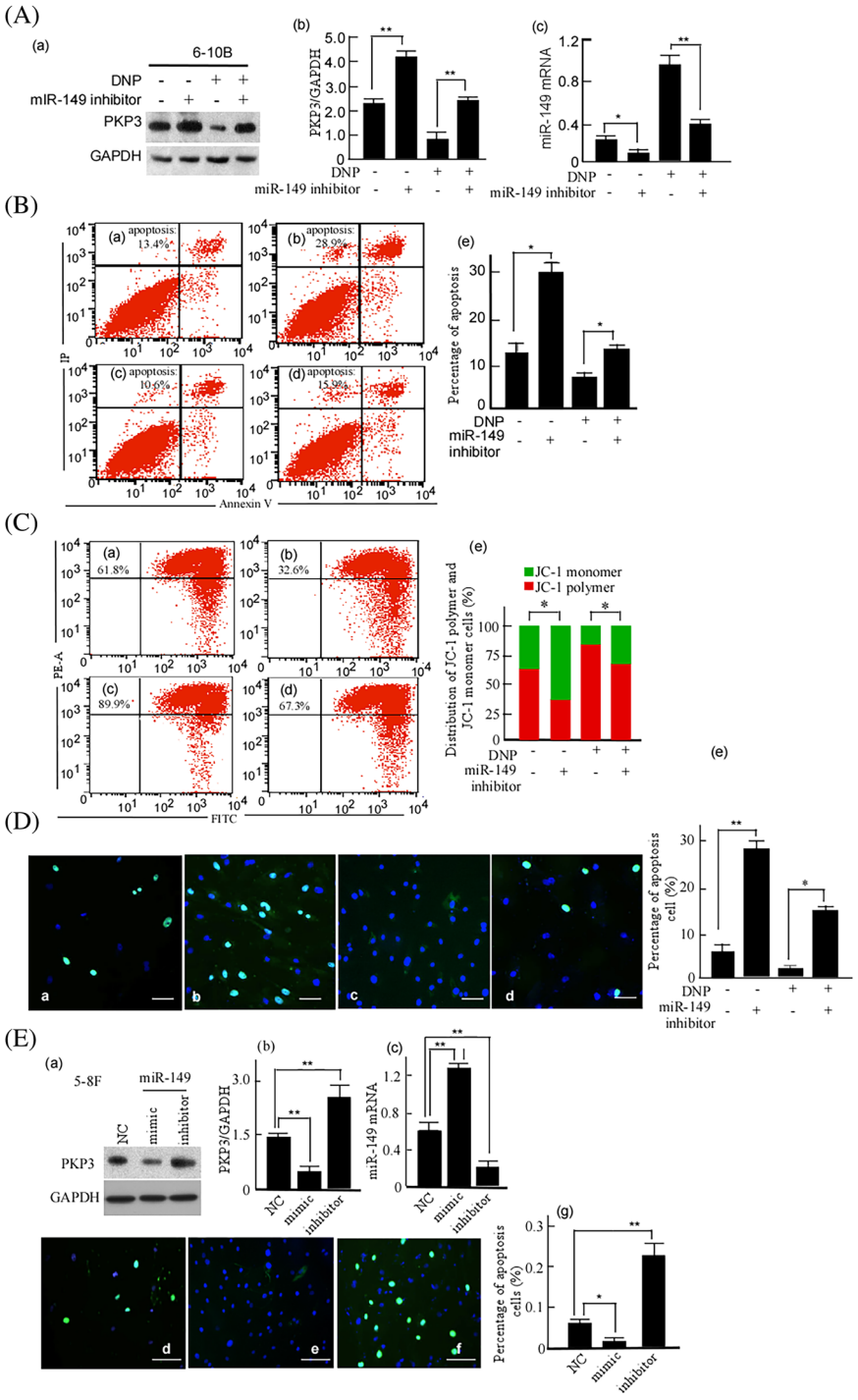

FIGURE 6 Cell apoptosis of 6-10B cells treated with miR-149 and DNP. A, 6-10B cells were treated with miR-149-inhibitor and/or DNP, PKP3 expressions were detected using Western-blotting (a). GAPDH was used as an internal control. The abundance ratio of PKP3 to GAPDH was counted (b), and miR-149 mRNA was detected using qRT-PCR (c). B, The treated cells were stained with Annexin V/PI staining, and then analyzed with flow cytometry. The apoptotic cells were counted. a, Blank control; b, Treatment with miR-149-inhibitor; c, Treatment with DNP; d, Treatment with miR-149-inhibitor plus DNP; e, Apoptosis rates of the treated cells were compared. C, The treated cells were stained with PEA/FITC staining, and Δψm in the treated cells was detected with flow cytometry. JC-1 monomer cells and JC-1 polymer cells were respectively counted. a, Blank control; b, Treatment with miR-149-inhibitor; c, Treatment with DNP; d, Treatment with miR-149-inhibitor plus DNP; e, JC-1 monomer and JC-1 polymer were compared. D, The treated 6-10B cells were stained with TUNEL kit, the positive cells were counted. a, Blank control; b, Treatment with miR-149-inhibitor; c, Treatment with DNP; d, Treatment with miR-149-inhibitor plus DNP; e, Apoptosis cells were comparatively analyzed. E, 5-8F cells were treated with miR-149 mimic or its inhibitor. PKP3 expression (a) and miR-149 mRNA (c) in the treated cells were detected, PKP3 expression was quantitatively compared (b). The treated cells were stained with FITC, apoptosis cells were detected. d, Blank control; e, Mimic; f, miR-149-inhibitor. Data are presented as means ± S.D. from three independent experiments statistically using the Student's *t* test. Scale bar, 10 μm; DNP, Dinitrosopiperazine; PKP3, Plakophilin3; Original magnification, ×400.*$P < 0.05$

cell was detected using fluorescence activated cell sorter (FACS) analysis. In viable cells with high Δψm, JC-1 monomers combine and form aggregates with intense red FL, which can be detected in FL2-A channel. In apoptotic cells with reduced or depolarized Δψm, JC-1 molecules remain as J-monomers with intense green FL detected in FL1-A channel.[54] Δψm was significantly reduced in 6-10B cells transfected with miR-149-inhibitor compared with the blank control. Δψm dramatically increased after DNP treatment, and this increase was attenuated by miR-149-inhibitor (Figure 6C; $P < 0.05$). TUNEL assay showed that TUNEL positive cells were increased in 6-10B cells transfected with miR-149-inhibitor (28.6 ± 5.7%) (Figure 6D-b, e; $P < 0.01$). DNP treatment markedly inhibited the number of TUNEL positive cells (3.6 ± 5.7%), while this inhibitory effect was removed by miR-149-inhibitor (17.2 ± 2.3%) (Figure 6D-d, e; $P < 0.05$). Moreover, TUNEL positive cells in 5-8F cells were decreased after miR-149 mimic transfection (2.3 ± 4.1%), and were increased in the miR-149-inhibitor group (17.2 ± 2.3%) (Figure 6E-f, g; $P < 0.05$). These above findings suggest that DNP-mediated apoptosis inhibition may be performed through miR-149.

3.7 | DNP-mediated miR-149 is involved in tube formation and induced F-actin expression

In the previous works, DNP has been proved to increase VEGF expression, and promotes NPC metastasis.[26] In the next study, we further confirm whether DNP-mediated miR-149 promotes angiogenesis formation. To determine the role of miR-149 on DNP-induced NPC angiogenesis, we first silenced miR-149 with special inhibitor or increased miR-149 expression with miR-149 mimic, and then treated with DNP, and observed the tube formation of HUVECs. We found that DNP greatly increased the tube formation of HUVECs (Figure 7B-b, e; $P < 0.05$), while miR-149-inhibitor reduced DNP-induced tube formation (Figure 7B-d, e; $P < 0.05$). The tube formation of 5-8F cells was decreased in the miR-149-inhibitor group (Figure 7D-c; $P < 0.05$), while it increased in the miR-149 mimic group (Figure 7D-b; $P < 0.05$). This suggests that DNP enhances angiogenesis formation through miR-149

Our previous works indicate that DNP induces NPC cell filopodia fiber formation,[25] and some studies reported a connection between actin cytoskeleton and ciliogenesis.[55] In this experiment, we also examined the possible contribution of actin dynamics in DNP-promoted ciliary growth. After being treated with DNP or miR-149-inhibitor, F-actin network organization of 6-10B was evaluated by F-actin immunostaining using fluorescence-labeled phalloidin. As being expected, DNP treatment profoundly increased the intensity of F-actin fluorescence (Figure 7B-h, j; $P < 0.05$), and such effect of DNP was greatly inhibited by miR-149-inhibitor (Figure 7B-i, j; $P < 0.05$). Moreover, F-actin in 5-8F cells was decreased in the miR-149-inhibitor group (Figure 7D-g, h; $P < 0.05$), and it was increased in the miR-149 mimic group (Figure 7D-f, h; $P < 0.05$). This indicated that DNP enhances ciliary growth through miR-149.

3.8 | DNP induces NPC metastasis through miR-149

To determine whether PKP3 downregulation mediated by miR-149 is associated with NPC metastasis in vivo, 5-8F cells treated with miR-149-inhibitor were injected into tail veins of nude mice, and cell metastasis was observed. The results showed that the metastatic node number and weight were significantly decreased when being treated with miR-149-inhibitor (Figure 8A-a, b), PKP3 expression increased in the metastatic tissues (Figure 8B-f). To further confirm that DNP induces NPC metastasis through miR-149 in vivo, the metastasis of 6-10B cells treated with DNP and miR-149-inhibitor was evaluated in nude mice. The results showed that the metastatic node number and weight were increased in 6-10B cells with DNP treatment (Figure 8B-a, b; $P < 0.05$), PKP3 expression was decreased (Figure 8B-g) and miR-149 was increased (Figure 8B-i; $P < 0.05$), while the metastasis was decreased when treated with miR-149-inhibitor (Figure 8B-a, b; $P < 0.05$), PKP3 expression was increased (Figure 8B-h) and miR-149 was decreased (Figure 8B-i; $P < 0.05$). These indicated that DNP exactly promotes NPC cell metastasis through regulating miR-149. Summary, in NPC metastasis DNP may upregulate miR-149 expression, downregulate PKP3 expression, increase NPC cell invasion, migration and adhesion, and finally promote NPC metastasis (Figure 9).

4 | DISCUSSION

In clinical settings, NPC is considered as a highly invasive and metastatic cancer. Both experimental studies and clinical assays indicated that DNP is an important factor of NPC metastasis.[25] In the previous works, we found that DNP regulates metastatic adhesion proteins, such as PKP3, clusterin, matrix metallo-proteinases (MMP), vascular endothelial growth factor (VEGF),[26,45] DNP also induces ezrin phosphorylation at Thr567,[25] HSP70-2 expression through increasing *HSP70*-2 transcription,[27] increases migration and invasion of cells, and promotes tumor metastasis, but their regulatory mechanisms are not entirely clear. In the present study, we probed whether DNP regulates the metastatic adhesion proteins through miRNA, and participates in NPC metastasis. miRNA sequencing was used to identify miRNAs expression in the cell with DNP treatment. miRNA sequencing data showed that miR-149 significantly increases in DNP-treated cells, next this results were confirmed by qRT-PCR. We speculate that miR-149 may participate in DNP-mediated NPC metastasis. miR-149 was reported to be down-regulated in various cancer, negatively correlated with cancer WHO grade.[34–37] Overexpression of miR-149 inhibits glioblastoma cell proliferation and migration.[37] miR-149 has also been proved to inhibit the proliferation and cell cycle progression in human gastric cancer.[38] However, the upregulated miR-149 was reported in NPC tissue[39] and cell lines.[40] miR-149 had been confirmed to promote the proliferation, invasion and migration of NPC cell,[41] but its regulating mechanism is not clear. Generally, miRNAs negatively modulate target genes by post-transcriptional regulation. To search for potential target genes of miR-149, the target scan analysis was used to calculate the binding of miR-149 with promoters of the above metastatic molecular genes, the data revealed that 3′-UTRs of *Pkp3* exists binding sites for

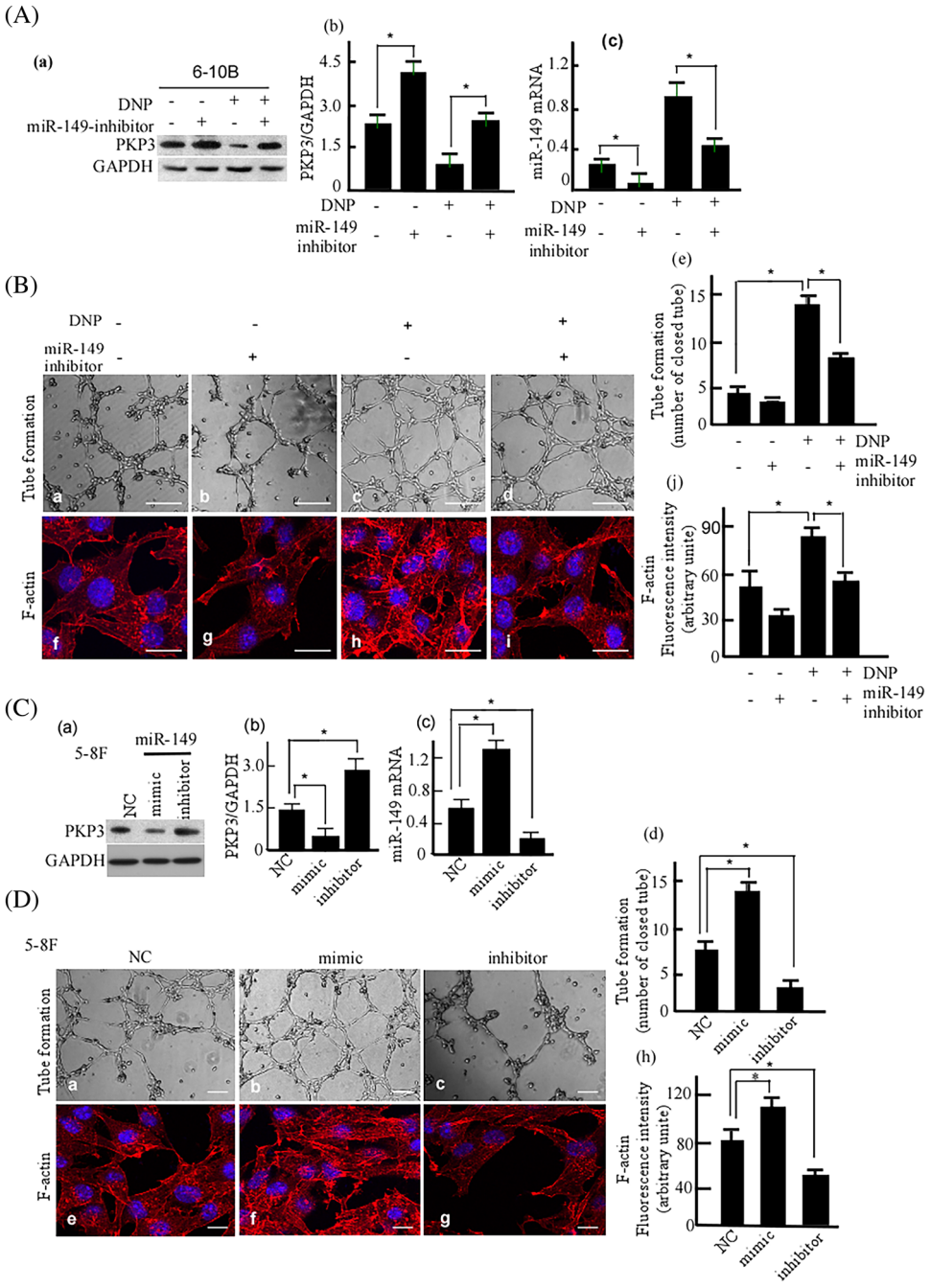

FIGURE 7 Tube formation and F-actin expression in 6-10B cells treated with miR-149 and DNP. A, 6-10B cells were treated with miR-149-inhibitor and/or DNP. PKP3 expressions were detected using Western-blotting (a). GAPDH was used as an internal control. The abundance ratio of PKP3 to GAPDH was counted (b). miR-149 mRNA was detected using qRT-PCR (c). B, Tube information of the treated cells was detected with the tube formation assay (a–d). The tubular structures formed in the matrigel were counted (e). a, Blank control; b, Treatment with miR-149-inhibitor; c, Treatment with DNP; d, Treatment with miR-149-inhibitor plus DNP; e, Tube formation was quantitively analyzed (e). scale bar, 5 μm; Original magnification, ×200. The treated cells were stained with F-actin immunostaining (f-i). The intensity of F-actin fluorescence was determined in 10 fields/well and divided by the cells stained with DAPI (j). f, Blank control; g, Treatment with miR-149-inhibitor; h, Treatment with DNP; i, Treatment with miR-149-inhibitor plus DNP; j, Tube formation was quantitively analyzed. scale bar, 20 μm; Original magnification, ×1000. C, 5-8F cells were treated with miR-149 mimic or its inhibitor. PKP3 (a) and miR-149 mRNA (c) were detected in the treated cells, PKP3 expression was quantitatively compared (b). D. Tube information of the treated 5-8F cells was detected (a, b, c). The tubular structures formed in the matrigel were counted (e). The treated 5-8F cells were stained with F-actin immunostaining (e-g). The intensity of F-actin fluorescence was determined in 10 fields/well and divided by the cells stained with DAPI (h). a, Blank control; b, Mimic; c, miR-149-inhibitor; d, Tube formation was quantitively analyzed; e, Blank control; f, Mimic; g, miR-149-inhibitor; h, Tube formation was quantitively analyzed. The experiments were performed in triplicate, and five fields from each chamber were counted and averaged. Data are presented as means ± S.D. from three independent experiments statistically using the Student's *t* test. DNP, Dinitrosopiperazine; PKP3, Plakophilin3. **P* < 0.05

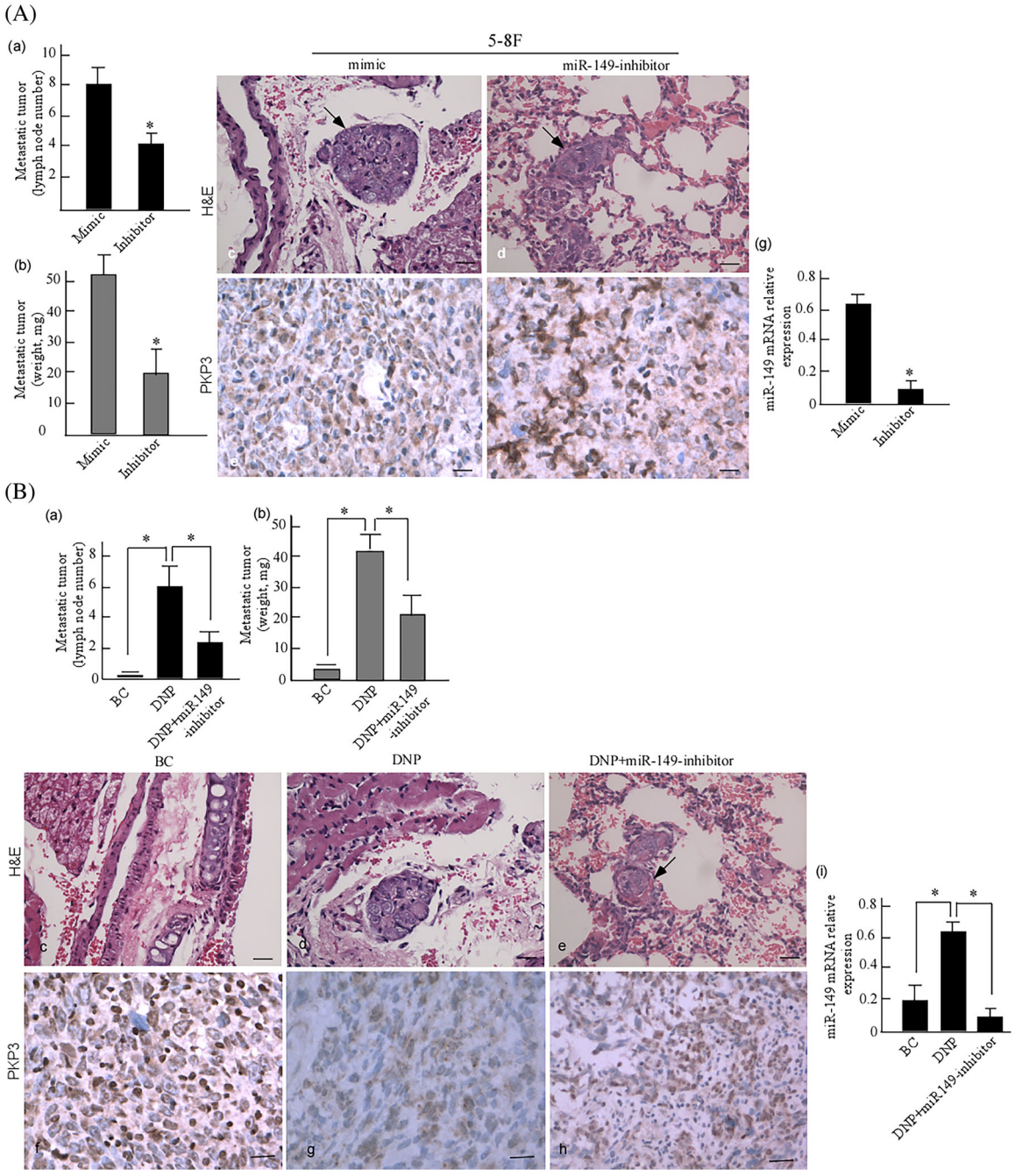

FIGURE 8 DNP-mediated 6-10B cell metastasis through miR-149 in vivo. A, 5-8F cells were transfected with miR-149-inhibitor or mimic, and then injected into nude mice through the tail vein. After 30 days, the mice were sacrificed and dissected, metastatic tumors were observed. The metastatic tumors were counted (a) and weighed (b). The tissue sections of metastatic tumors were made, and the sections were stained with hematoxylin and eosin (H&E) (c, d). PKP3 in the metastatic tumor was detected using immunohistochemistry (IHC) (e, f), and miR-149 was detected using qRT-PCR (g). Scale bar, 100 μm (*$P < 0.05$). B, 6-10B cells were transfected with miR-149-inhibitor and injected into nude mice, and then randomly divided into two groups. One group was abdominally injected with DNP. The other group was injected with saline, served as a blank control (BC). After 30 days, the metastatic tumors were counted (a) and weighed (b). The tumor sections were stained with H&E (c-e). PKP3 in the tumor was detected using IHC (f-h), and miR-149 was detected using qRT-PCR (i). Arrows, metastatic node. In H&E, scale bar, 20 μm; Original magnification, ×200. In IHC, scale bar, 100 μm; DNP, Dinitrosopiperazine; PKP3, Plakophilin3.Original magnification, ×400

miR-149. The luciferase assays using *Pkp3* 3′-UTR reporter plasmids showed that *Pkp3* transcription decreased when miR-149 transfection. These results suggest that miR-149 negatively regulates PKP3 expression. In our previous works, we found that NPC cell with high metastatic ability has a low PKP3 expression.[45] Recent studies have revealed that PKP3 loss is associated with tumor progression and metastasis in oral cavity and colon tumors.[43,44] Clinical assay showed that NPC tissues display a significant high miR-149 and low PKP3

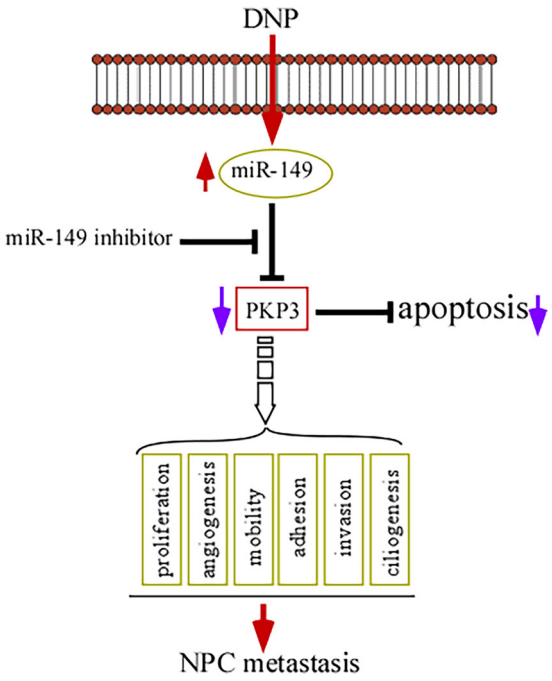

FIGURE 9 Schematic illustration of DNP-promoted NPC metastasis through miR-149. DNP induces miR-149 and decreases PKP3 expression, increases cell proliferation and decreases apoptosis, further enhances invasion, migration, adhesion, angiogenesis, and ciliogenesis of NPC cancer, and finally promotes NPC metastasis. DNP, Dinitrosopiperazine; PKP3, Plakophilin3

expressions. These results indicated that miR-149 and PKP3 play an important role in NPC metastasis. Based on the above, we speculate that miR-149 negatively regulating PKP3 participates in NPC metastasis.

Further, experiment studies showed that DNP could induce miR-149 expression and inhibit PKP3 expression, and increase NPC cell migration, invasion, and adhesion. However, miR-149 was reported to be downregulated in various cancer and be a tumor suppressor,[34–37] but an upregulated miR-149 level was reported in other tumors including NPC,[39,40] and miR-149 promotes the proliferation, invasion, and migration of NPC cell lines.[41] In the present study, we found overexpression of miR-149 along with PKP3 lowexpression in NPC tissues and cell, and downregulation of miR-149 resulting in the increment of PKP3 expression. And the DNP-mediated PKP3 decrease was eliminated by miR-149 in NPC cells. This suggests that DNP may reduce PKP3 expression through upregulating miR-149.

It has early been reported that miR-149 family mediates cell apoptosis repression and proliferation increase.[53,56] In our study, FACS analysis and TUNEL assay showed that miR-149 negatively regulating PKP3 participates in DNP-mediated cell proliferation and apoptosis inhibition. Additionally, DNP also induces angiogenesis in NPC cells.[26] It has been documented that ciliogenesis and angiogenesis are critical factors of cancer metastasis.[57,58] Lastly, we also examined actin dynamics in DNP-promoted ciliary growth and the role of miR-149 in DNP-induced NPC angiogenesis. Our data showed that DNP regulated ciliary growth and angiogenesis through increasing miR-149 level. In summary, DNP, a specific pathogenic factors for NPC, was identified to downregulate PKP3 expression through elevating miR-149, and induce cell proliferation, migration, invasion, and adhesion, and finally promotes NPC metastasis (Figure 8). This provides a new avenue for NPC metastasis research and novel immunotherapeutic strategy.

ACKNOWLEDGMENTS

We thank Dr Daofa Tian and Prof Tieying Li for kindly providing DNP. We appreciate the contributions and helpful discussion of various members in Clinical Laboratory of Zhuhai Hospital, Jinan University. And This work was supported in part by the National Natural Science Foundation of China (81372282, 81872226, 81402368, 81402265, 81502346), Guangdong Provincial Science and Technology Project Foundation (2017A020215136), Guangdong Natural Science Foundation (S2013010013360), China Postdoctoral Science Foundation funded project (2016M592580).

CONFLICT OF INTEREST

The authors state no conflict of interest.

ORCID

Faqing Tang http://orcid.org/0000-0003-0279-2956

REFERENCES

1. Wei WI, Sham JST. Nasopharyngeal carcinoma. *Lancet*. 2005;365:2041–2054.
2. Cao SM, Simons MJ, Qian CN. The prevalence and prevention of nasopharyngeal carcinoma in China. *Chin J Cancer*. 2011;30:114–119.
3. Simons MJ. Nasopharyngeal carcinoma as a paradigm of cancer genetics. *Chin J Cancer*. 2011;30:79–84.
4. Chan. Nasopharyngeal carcinoma. *Ann Oncol*. 2010;21:vii308–vii312.
5. Chua DT, Sham JS, Kwong DL, Wei WI, Au GK, Choy D. Locally recurrent nasopharyngeal carcinoma: treatment results for patients with computed tomography assessment. *Int J Radiat Oncol Biol Phys*. 1998;41:379–386.
6. Al-Sarraf M, LeBlanc M, Giri PG, et al. Chemoradiotherapy versus radiotherapy in patients with advanced nasopharyngeal cancer: phase III randomized Intergroup study 0099. *J Clin Oncol*. 1998;16:1310–1317.
7. Liebowitz D. Nasopharyngeal carcinoma: the Epstein-Barr virus association. *Semin Oncol*. 1994;21:376–381.
8. Shao JY, Zeng WF, Zeng YX. Molecular genetic progression on nasopharyngeal carcinoma. *Ai Zheng*. 2002;21:1–10.
9. Yu MC. Diet and nasopharyngeal carcinoma. *FEMS Microbiol Immunol*. 1990;2:235–242.
10. Henderson BE, Louie E. Discussion of risk factors for nasopharyngeal carcinoma. *IARC Sci Publ*. 1978;20:251–260.
11. Yu MC, Ho JH, Lai SH, Henderson BE. Cantonese-style salted fish as a cause of nasopharyngeal carcinoma: report of a case-control study in Hong Kong. *Cancer Res*. 1986;46:956–961.
12. Yu MC, Huang TB, Henderson BE. Diet and nasopharyngeal carcinoma: a case-control study in Guangzhou. *China. Int J Cancer*. 1989;43:1077–1082.

13. Armstrong RW, Imrey PB, Lye MS, Armstrong MJ, Yu MC, Sani S. Nasopharyngeal carcinoma in Malaysian Chinese: salted fish and other dietary exposures. *Int J Cancer*. 1998;77:228–235.
14. Yuan JM, Wang XL, Xiang YB, Gao YT, Ross RK, Yu MC. Preserved foods in relation to risk of nasopharyngeal carcinoma in Shanghai. *China. Int J Cancer*. 2000;85:358–363.
15. Zou J, Sun Q, Akiba S, et al. A case-control study of nasopharyngeal carcinoma in the high background radiation areas of Yangjiang. *China. J Radiat Res (Tokyo)*. 2000;41:53–62.
16. Jia WH, Luo XY, Feng BJ, et al. Traditional Cantonese diet and nasopharyngeal carcinoma risk: a large-scale case-control study in Guangdong, China. *BMC Cancer*. 2010;10:446.
17. Zou XN, Lu SH, Liu B. Volatile N-nitrosamines and their precursors in Chinese salted fish—a possible etological factor for NPC in China. *Int J Cancer*. 1994;59:155–158.
18. Poirier S, Hubert A, de-The G, Ohshima H, Bourgade MC, Bartsch H. Occurrence of volatile nitrosamines in food samples collected in three high-risk areas for nasopharyngeal carcinoma. *IARC Sci Publ*. 1987; 415–419.
19. Lijinsky W, Kovatch RM. Carcinogenic effects in rats of nitrosopiperazines administered intravesically: possible implications for the use of piperazine. *Cancer Lett*. 1993;74:101–103.
20. Jakszyn P, Gonzalez CA. Nitrosamine and related food intake and gastric and oesophageal cancer risk: a systematic review of the epidemiological evidence. *World J Gastroenterol*. 2006;12:4296–4303.
21. Gallicchio L, Matanoski G, Tao XG, et al. Adulthood consumption of preserved and nonpreserved vegetables and the risk of nasopharyngeal carcinoma: a systematic review. *Int J Cancer*. 2006;119:1125–1135.
22. Huang DP, Ho JH, Saw D, Teoh TB. Carcinoma of the nasal and paranasal regions in rats fed Cantonese salted marine fish. *IARC Sci Publ*. 1978;315–328.
23. Yu MC, Nichols PW, Zou XN, Estes J, Henderson BE. Induction of malignant nasal cavity tumours in Wistar rats fed Chinese salted fish. *Br J Cancer*. 1989;60:198–201.
24. Zheng X, Luo Y, Christensson B, Drettner B. Induction of nasal and nasopharyngeal tumours in Sprague-Dawley rats fed with Chinese salted fish. *Acta Otolaryngol*. 1994;114:98–104.
25. Tang F, Zou F, Peng Z, et al. N,N'-dinitrosopiperazine-mediated ezrin protein phosphorylation via activation of Rho kinase and protein kinase C is involved in metastasis of nasopharyngeal carcinoma 6-10B cells. *J Biol Chem*. 2011;286:36956–36967.
26. Kong Y, Zou S, Yang F, et al. RUNX3-mediated up-regulation of miR-29b suppresses the proliferation and migration of gastric cancer cells by targeting KDM2A. *Cancer Lett*. 2016;381:138–148.
27. Cheng YJ, Tang FY, Bao CJ, et al. Spatial analyses of typhoid fever in Jiangsu province, People's Republic of China. *Geospat Health*. 2013;7: 279–288.
28. Ambros V. The functions of animal microRNAs. *Nature*. 2004;431: 350–355.
29. Bartel DP. MicroRNAs: target recognition and regulatory functions. *Cell*. 2009;136:215–233.
30. Lee KT, Tan JK, Lam AK, Gan SY. MicroRNAs serving as potential biomarkers and therapeutic targets in nasopharyngeal carcinoma: a critical review. *Crit Rev Oncol Hematol*. 2016;103:1–9.
31. Bruce JP, Liu FF. MicroRNAs in nasopharyngeal carcinoma. *Chin J Cancer*. 2014;33:539–544.
32. Brunetti O, Russo A, Scarpa A, et al. MicroRNA in pancreatic adenocarcinoma: predictive/prognostic biomarkers or therapeutic targets? *Oncotarget*. 2015;6:23323–23341.
33. Rachagani S, Macha MA, Heimann N, et al. Clinical implications of miRNAs in the pathogenesis, diagnosis and therapy of pancreatic cancer. *Adv Drug Deliv Rev*. 2015;81:16–33.
34. Wong TS, Liu XB, Wong BY, Ng RW, Yuen AP, Wei WI. Mature miR-184 as potential oncogenic microRNA of squamous cell carcinoma of tongue. *Clin Cancer Res*. 2008;14:2588–2592.
35. Liu H, Brannon AR, Reddy AR, et al. Identifying mRNA targets of microRNA dysregulated in cancer: with application to clear cell Renal Cell Carcinoma. *BMC Syst Biol*. 2010;4:51.
36. Schaefer A, Jung M, Mollenkopf HJ, et al. Diagnostic and prognostic implications of microRNA profiling in prostate carcinoma. *Int J Cancer*. 2010;126:1166–1176.
37. Li D, Chen P, Li XY, et al. Grade-specific expression profiles of miRNAs/mRNAs and docking study in human grade I-III astrocytomas. *OMICS*. 2011;15:673–682.
38. Wang Y, Zheng X, Zhang Z, et al. MicroRNA-149 inhibits proliferation and cell cycle progression through the targeting of ZBTB2 in human gastric cancer. *PLoS ONE*. 2012;7:e41693.
39. Luo Z, Zhang L, Li Z, et al. An in silico analysis of dynamic changes in microRNA expression profiles in stepwise development of nasopharyngeal carcinoma. *BMC Med Genomics*. 2012;5:3.
40. Huang GL, Lu Y, Pu XX, et al. Association study between miR-149 gene polymorphism and nasopharyngeal carcinoma. *Biomed Rep*. 2013;1: 599–603.
41. Luo Z, Zhang L, Li Z, et al. MiR-149 promotes epithelial-mesenchymal transition and invasion in nasopharyngeal carcinoma cells. *J Cent South Univ (Med Sci)*. 2011;36:604–609.
42. Bonne S, van Hengel J, Nollet F, Kools P, van Roy F. Plakophilin-3, a novel armadillo-like protein present in nuclei and desmosomes of epithelial cells. *J Cell Sci*. 1999;112:2265–2276.
43. Aigner K, Descovich L, Mikula M, et al. The transcription factor ZEB1 (deltaEF1) represses Plakophilin 3 during human cancer progression. *FEBS Lett*. 2007;581:1617–1624.
44. Papagerakis S, Shabana AH, Depondt J, Gehanno P, Forest N. Immunohistochemical localization of plakophilins (PKP1, PKP2, PKP3, and p0071) in primary oropharyngeal tumors: correlation with clinical parameters. *Hum Pathol*. 2003;34:565–572.
45. Li Y, Liu N, Huang D, et al. Proteomic analysis on N, N'-dinitrosopiperazine-mediated metastasis of nasopharyngeal carcinoma 6-10B cells. *BMC Biochem*. 2012;13:13–25.
46. Li Y, Lu J, Peng Z, et al. N,N'-dinitrosopiperazine-mediated AGR2 is involved in metastasis of nasopharyngeal carcinoma. *PLoS ONE*. 2014;9:e92081.
47. Wang ZM, Xue W, Dong CJ, et al. A comparative miRNAome analysis reveals seven fiber initiation-related and 36 novel miRNAs in developing cotton ovules. *Mol Plant*. 2012;5:889–900.
48. Zhang JP, Zhang H, Wang HB, et al. Down-regulation of Sp1 suppresses cell proliferation, clonogenicity and the expressions of stem cell markers in nasopharyngeal carcinoma. *J Transl Med*. 2014;12:222.
49. Guo H, Xia B. Collapsin response mediator protein 4 isoforms (CRMP4a and CRMP4b) have opposite effects on cell proliferation, migration, and invasion in gastric cancer. *BMC Cancer*. 2016;16: 565.
50. Zhou Y, Zhao RH, Tseng KF, et al. Sirolimus induces apoptosis and reverses multidrug resistance in human osteosarcoma cells in vitro via increasing microRNA-34b expression. *Acta Pharmacol Sin*. 2016;37:519–529.
51. Li J, Li G. Cell cycle regulator ING4 is a suppressor of melanoma angiogenesis that is regulated by the metastasis suppressor BRMS1. *Cancer Res*. 2010;70:10445–10453.
52. Fujii T, Shimada K, Tatsumi Y, Fujimoto K, Konishi N. Syndecan-1 responsive microRNA-126 and 149 regulate cell proliferation in prostate cancer. *Biochem Biophys Res Commun*. 2015;456:183–189.
53. Chen Y, Zhao J, Luo Y, Wang Y, Jiang Y. Downregulated expression of miRNA-149 promotes apoptosis in side population cells sorted from the TSU prostate cancer cell line. *Oncol Rep*. 2016;36: 2587–2600.
54. Vermes I, Haanen C, Reutelingsperger C. Flow cytometry of apoptotic cell death. *J Immunol Methods*. 2000;243:167–190.
55. Kim J, Lee JE, Heynen-Genel S, et al. Functional genomic screen for modulators of ciliogenesis and cilium length. *Nature*. 2010;464: 1048–1051.

56. Fan SJ, Li HB, Cui G, et al. MiRNA-149 promotes cell proliferation and suppresses apoptosis by mediating JunB in T-cell acute lymphoblastic leukemia. *Leuk Res*. 2016;41:62–70.
57. Gibbs BC, Damerla RR, Vladar EK, et al. Prickle1 mutation causes planar cell polarity and directional cell migration defects associated with cardiac outflow tract anomalies and other structural birth defects. *Biol Open*. 2016;5:323–335.
58. Jiang H, Chen C, Sun Q, et al. The role of semaphorin 4D in tumor development and angiogenesis in human breast cancer. *Onco Targets Ther*. 2016;9:5737–5750.

How to cite this article: Li Y, Ju K, Wang W, et al. Dinitrosopiperazine-decreased PKP3 through upregulating miR-149 participates in nasopharyngeal carcinoma metastasis. *Molecular Carcinogenesis*. 2018;57:1763–1779. https://doi.org/10.1002/mc.22895